

Cyclo-*meta*-phenylene Revisited: Nickel-Mediated Synthesis, Molecular Structures, and Device Applications

Jing Yang Xue,[†] Koki Ikemoto,[‡] Norihisa Takahashi,[†] Tomoo Izumi,^{‡,¶} Hideo Taka,^{‡,¶} Hiroshi Kita,[¶] Sota Sato,^{*,†,‡} and Hiroyuki Isobe^{*,†,‡}

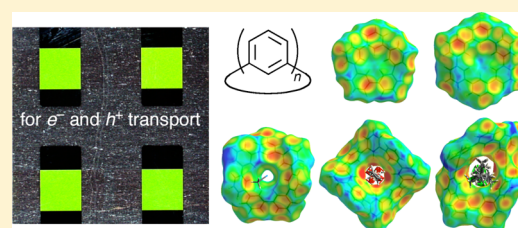
[†]Advanced Institute for Materials Research and Department of Chemistry, Tohoku University, Aoba-ku, Sendai 980-8578, Japan

[‡]Isobe Degenerate π -Integration Project, ERATO JST, Aoba-ku, Sendai 980-8577, Japan

[¶]Advanced Layer Company, Konica Minolta, Ishikawa-cho, Hachioji 192-8505, Japan

S Supporting Information

ABSTRACT: From a one-pot nickel-mediated Yamamoto-type coupling reaction of *m*-dibromobenzene, five congeners of [*n*]cyclo-*meta*-phenylenes were synthesized and fully characterized. The [*n*]cyclo-*meta*-phenylenes possessed a commonly shared arylene unit and intermolecular contacts but varied in packing structures in the crystalline solid state. Columnar assembly of larger congeners yielded nanoporous crystals with carbonaceous walls to capture minor protic or aliphatic solvent molecules. The concise and scalable synthesis allowed exploration of the macrocyclic hydrocarbons as bipolar charge carrier transport materials in organic light-emitting diode devices.



INTRODUCTION

The chemistry of cyclophenylene hydrocarbons has gained renewed interest in recent years.¹ The field began with the ortho-linked macrocyclic hydrocarbons, cyclo-*ortho*-phenylenes (COP), in the 1940s^{2,3} and experienced another wave of interest with the arrival of cyclo-*meta*-phenylenes (CMP) in the 1960s.^{4–7} After several decades, the remaining challenge, cyclo-*para*-phenylenes (CPP), was synthesized in the 2000s and revived the subject with new scopes related to nanocarbon molecules.⁸ We independently entered this field by introducing [*n*]cyclo-2,7-naphthylenes ([*n*]CNAP) through the extension of the π -systems in the macrocyclic hydrocarbons.^{9,10} In addition to our initial interest in the molecules as defective graphene models, we were intrigued by the potential of macrocyclic hydrocarbons in organic materials science. Because it lacks thermally labile or electronically biased substituents on its cyclic hydrocarbon skeleton, the molecule possesses an extremely high thermal stability and functions as a bipolar charge transporting material in organic light-emitting diode (OLED) devices. The degenerate π -systems embedded in the strain-free macrocyclic hydrocarbon were thus beneficial for materials applications. We therefore hypothesized that [*n*]CMP with similar but simpler cyclic hydrocarbon structures would be an ideal target for materials applications if we could establish a scalable and concise synthesis. We herein report a one-pot, concise synthesis of [*n*]CMP from *m*-dibromobenzene. A nickel-mediated macrocyclization method enabled the preparation of major [*n*]CMP with a yield of 1 g. Structural features of [*n*]CMP in the solid state have been revealed by X-ray diffraction and Hirshfeld surface analyses.¹¹ The hydrocarbon macrocycles, [*n*]CMP, show an excellent level of thermal

stability and functions as bipolar charge carrier transporting materials in OLED devices. A higher external quantum efficiency of [*n*]CMP devices was found, when compared with [*n*]CNAP devices.

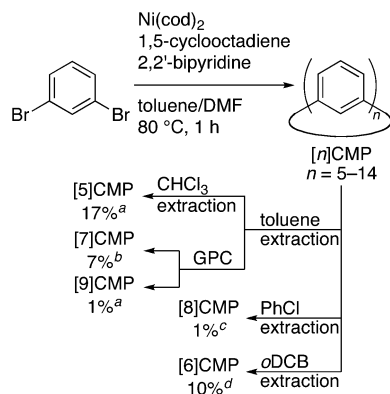
RESULTS AND DISCUSSION

The synthesis of [*n*]CMP was renovated simply by adopting an appropriate coupling reaction. The original one-pot synthesis of [*n*]CMP hydrocarbons was reported by Staab, who recorded a yield of 1.1% for the major congener of $n = 6$ from *m*-dibromobenzene via a copper-mediated coupling reaction with the corresponding Grignard reagent. Although the synthesis was improved by multistep coupling routes, the overall yield of the major congener, [6]CMP, from *m*-dibromobenzene was only improved to 5.8%.^{4,12–15} Through our experience with [*n*]CNAP synthesis,⁹ we hypothesized that replacing the labile Grignard reagent with an electroneutral reagent should be an improvement. We thus examined a one-pot macrocyclization reaction, a Yamamoto-type coupling reaction,¹⁶ of *m*-dibromobenzene with Ni(cod)₂/2,2'-bipyridine in a mixture of toluene and DMF (Scheme 1) and found that the coupling reaction indeed proceeded to afford a mixture of [*n*]CMP.¹⁷ After quenching the reaction with aqueous HCl, we detected [*n*]CMP with $n = 5, 7, 9–14$ in toluene solution and [6]- and [8]CMP in precipitates (Figure S1, Supporting Information).

The isolation of representative congeners was successfully performed using a combination of extraction, chromatography, and crystallization (Scheme 1).⁹ We first isolated [5]-, [7]-, and

Received: August 18, 2014

Published: September 29, 2014

Scheme 1. Synthesis of $[n]$ CMP

^aIsolated yield after subsequent purification by recrystallization from toluene. ^bIsolated yield after subsequent purification by recrystallization from $\text{CHCl}_3/\text{MeCN}$. ^cIsolated yield after subsequent purification by recrystallization from PhCl/MeOH . ^dIsolated yield after subsequent purification by recrystallization from *o*DCB and sublimation.

[9]CMP from the toluene solution after the reaction. After the removal of toluene from the crude solution, [5]CMP was extracted with CHCl_3 and obtained in 17% yield after recrystallization from toluene. From the residual solid was obtained [7]- and [9]CMP in 7% and 1% yields, respectively, after gel permeation chromatography and recrystallization. We then isolated [6]- and [8]CMP from the precipitates of the reaction: [8]CMP was extracted with PhCl and isolated in 1% yield after recrystallization, and [6]CMP was subsequently extracted with *o*-dichlorobenzene (*o*DCB) and obtained in 10% yield after recrystallization and sublimation. The present method is concise and scalable to afford two major compounds, i.e., [5]- and [6]CMP, in 1.10 g (17% yield) and 0.667 g (10% yield), respectively, from 20 g of *m*-dibromobenzene.

Features of molecular structures of $[n]$ CMP in the crystalline solid state were revealed by X-ray diffraction and Hirshfeld surface analyses of single crystals.¹⁸ The Hirshfeld surfaces mapped with d_e parameters are shown in Figure 1.^{11,19,20} The d_e color mapping shows the intermolecular distance from the surface to the external atoms and thus allows for the extraction of information on the atomic contacts with the inner molecule graphically. The red-orange dots that predominantly cover the surfaces of $[n]$ CMP molecules show the presence of short atomic contacts with the hydrogen atoms of neighboring molecules (Figure 1a). Thus, $\text{CH}-\pi$ contacts, a typical and ubiquitous feature for aromatic hydrocarbons, commonly predominate in the intermolecular contacts in the molecular packing, which can also be observed in the small surface area of the carbon-carbon contacts (C-C area in Figure 1a, and Figure S13, Supporting Information).²¹

Possessing three-dimensional molecular shapes with larger macrocyclic openings, the larger congeners, [7]-, [8]-, and [9]CMP, accommodated solvent molecules in the single crystals. The encapsulated solvent molecules were acetonitrile (MeCN) for [7]CMP, water (H_2O), and methanol (MeOH) for [8]CMP and hexane and chloroform (CHCl_3) for [9]CMP. The corresponding Hirshfeld surfaces of the encapsulated molecules are shown in Figure 1b. Note that the Hirshfeld surface of the encapsulated molecules serves as an inspection probe for the surrounding environment and provides information about interacting contacts. The small macrocycle, [7]CMP, encapsulated the solvent molecules in the void space

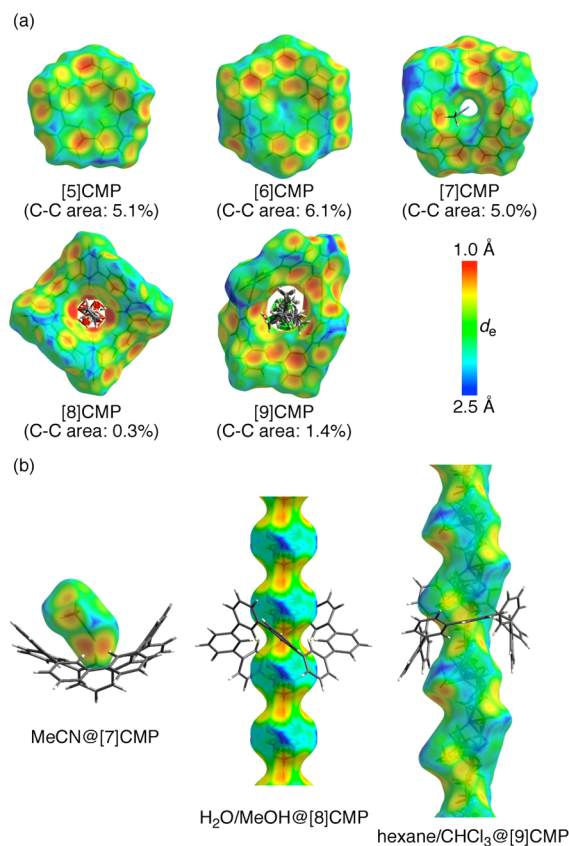


Figure 1. Molecular structures in tube models and the transparent Hirshfeld surfaces of $[n]$ CMP. (a) Top view: Hirshfeld surfaces with d_e mapping on $[n]$ CMP molecules. Solvent molecules were found as follows: one MeCN molecule with 100% occupancy for [7]CMP, two H_2O molecules with 50% and 37.5% occupancies, and one MeOH molecule with 12.5% occupancy for [8]CMP and two hexane molecules with 39% and 14% occupancies and one CHCl_3 molecule with 34% occupancy for [9]CMP. Except for [7]CMP, single crystallographically independent macrocyclic structures were found in the crystals. Among the crystallographically independent molecules of [7]CMP in a unit cell, one bearing a direct contact with MeCN was shown. The other molecule possessed a similar structure without large deviations in dihedral angles. (b) Side view: Hirshfeld surfaces with d_e mapping on the encapsulated solvent molecules. See Supporting Information for additional data.

of the crystal, and each MeCN molecule was separately located in the isolated voids surrounded by phenylene units. Conversely, solvent molecules in [8]- and [9]CMP were captured in a one-dimensional pore of the crystal. To our surprise, the encapsulated molecules in [8]- and [9]CMP were minor components in the recrystallization media: methanol and hexane were introduced in the recrystallization media as poor solvents through vapor diffusion, and water was not intentionally introduced but was present in the other solvents or atmosphere. Constructed by columnar assembly and a resultant array of macrocyclic openings of CMP molecules, the pore is surrounded by hydrogen and sp^2 -carbon atoms of the macrocycles. An apparent difference in the pore walls of [8]- and [9]CMP can be graphically understood by inspecting the Hirshfeld surface, showing the sp^2 -carbon contacting areas (Figure S14, Supporting Information): [8]CMP possessed periodic beltlike patches of carbonaceous areas, whereas [9]CMP possessed consecutive carbonaceous streaks through the pore. It is interesting to note that minor protic molecules

such as water or methanol were entrapped in the hydrophobic belts, and minor aliphatic molecules such as hexane were aligned in the hydrophobic streaks. The present observation may thus indicate that the crystalline pore walled by sp^2 -carbon atoms may have unique and favorable interactions with protic or aliphatic molecules. Similar interactions have previously been observed in the inner spaces of carbon nanotubes.^{22,23}

Before the fabrication of OLED devices, several fundamental properties of $[n]$ CMP were studied, which revealed favorable characters of the macrocyclic hydrocarbons for materials applications. The macrocycles were all transparent in the visible light region, which is favorable for optoelectronic applications: the absorption maxima of $[n]$ CMP were commonly found to be approximately 250 nm (Table 1) and

Table 1. Fundamental Properties of $[n]$ CMP

	λ_{\max}^a (nm)	T_d^b (°C)	strain ^c (kcal/mol)
[5]CMP	252	358	23
[6]CMP	250	451	1.3
[7]CMP	250	440	3.6
[8]CMP	246	449	1.6
[9]CMP	248	480	6.3

^aMeasurement of UV–vis spectra was carried out in $CHCl_3$. See Supporting Information for the spectra. ^bThe decomposition temperature was measured by thermogravimetric analysis with ca. 2 mg of specimen under a helium atmosphere. ^cStrain energies were theoretically estimated by DFT calculations of homodesmotic reactions with B3LYP/6-31G(d,p).⁹ See Supporting Information for details.

did not deviate significantly from monomeric benzene (Figure S15, Supporting Information).²⁴ Thermal robustness was revealed by thermogravimetric (TG) analysis (See also Figure S16, Supporting Information). Although the decomposition temperature (T_d , onset) tended to be lower than that of $[n]$ CNAP with naphthylene units, all of the $[n]$ CMP molecules survived above 350 °C, and the fabrication of devices through sublimation was secured.²⁵ Although the T_d values qualitatively depended on the strain energy of the macrocycles (Table 1), other factors such as packing structures may have influenced the decomposition temperatures.²⁶

Finally, we investigated the application of CMP in OLED devices. Using two major congeners, [5]- and [6]CMP, in charge carrier transport layers, we fabricated OLED devices through sublimation. The other components and layer settings were the same as those of previous $[n]$ CNAP devices,⁹ and the phosphorescent OLED devices were fabricated with the following configurations: ITO (indium tin oxide; 100 nm)/PEDOT:PSS (poly(ethylenedioxy)thiophene:polystyrenesulfonate; 20 nm)/HTL (hole transport layer, 20 nm)/CBP: [Ir(ppy)₃, 6%] (4,4'-N,N'-dicarbazole biphenyl:tris(2-phenylpyridine)iridium; 40 nm)/BCP (bathocuproine, 10 nm)/ETL (electron transport layer, 30 nm)/LiF (0.5 nm)/Al (110 nm) (Figure S18, Supporting Information).²⁷ As shown in Table 2, [5]- and [6]CMP were active both in the hole- and electron-transport layers of the OLED devices, and the inherent bipolar nature of hydrocarbon macrocycles as charge carrier transporters was confirmed for these macrocycles possessing fundamental phenylene units. The hydrocarbon macrocycles, however, preferred hole-transport to electron-transport: a high performance of approximately 13% in external quantum efficiency (EQE) was recorded with CMP in HTL (devices C

Table 2. Device Performance of OLED at a Constant Current Density of 2.5 mA·cm⁻²

device	HTL	ETL	DV ^a (V)	EQE ^b (%)
A ^c	α -NPD	Alq ₃	6.6	10.7
B ^c	[6]CNAP	Alq ₃	7.5	12.6
C	[5]CMP	Alq ₃	8.7	13.9
D	[6]CMP	Alq ₃	8.6	13.2
E ^c	α -NPD	[6]CNAP	6.4	10.5
F	α -NPD	[5]CMP	6.3	5.1
G	α -NPD	[6]CMP	11.7	4.9

^aDriving voltage. ^bExternal quantum efficiency. ^cReference 9.

and D), which surpassed that of [6]CNAP with naphthylene units (device B).⁹ The devices with $[n]$ CMP in ETL showed a lower EQE of approximately 5% (devices F and G). Theoretical analysis of the reorganization energies through the carrier transport processes showed that the structural rigidity of $[n]$ CMP was pronounced in the hole transport but was weakened in the electron transport (Table S7, Supporting Information). This theoretical result may partly explain the relatively lower performance of $[n]$ CMP in ETL. The higher driving voltage (DV) for the OLED devices may be ascribed to the higher LUMO levels and lower HOMO levels (Figure S17, Supporting Information), although the relatively large difference in the DV values for CMP/ETL devices (devices F and G) cannot be readily understood. Other factors such as packing structures in the thin layers are currently under investigation.

In summary, we have developed a concise, one-pot synthesis method for hydrocarbon macrocycles, $[n]$ CMP. The simple Ni-mediated coupling reaction of *m*-dibromobenzene under diluted conditions was suitable for the synthesis of a series of the macrocycles in moderate yields. The present synthesis allowed for the structural identification of a series of $[n]$ CMP with $n = 5-9$, including their crystalline solid-state structures. Despite the common intermolecular CH– π contacts in the packing, the crystalline structures displayed a diverse range of packing structures, and larger macrocycles showed the presence of voids or pores to encapsulate small molecules. The unique nanopores in [8]- and [9]CMP, particularly with the sp^2 -carbon walls of phenylenes, may allow us to understand the characteristics of π -rich carbonaceous pores. The applicability of $[n]$ CMP in OLED devices was realized by both a scalable synthesis and the thermal robustness for sublimation, which revealed the bipolar charge carrier transporting ability of the hydrocarbon macrocycles. This study indicated a high potential for cyclophenylenes in materials research. A difference in the preference for the charge carriers between two closely related macrocyclic hydrocarbons, $[n]$ CMP and $[n]$ CNAP, may indicate a sophisticated fine-tuning of electronics in hydrocarbon materials, for instance, through a molecular design via cross-coupling routes. Combining the preceding knowledge on polyphenylene materials,^{28,29} structural designs of hydrocarbon materials with discrete molecular structures may be of great interest for organic electronic applications in the future.³⁰ A combined design of phenylene macrocyclic structures, for instance, with supramolecular nanopores for the encapsulation of modular substances may be explored.^{31–33}

EXPERIMENTAL SECTION

General. Gel permeation chromatography (GPC) was performed with JAIGEL 1H, 2H, and 2.SH polystyrene columns. The analysis of product purity was performed by high pressure liquid chromatography

(HPLC) using a Cosmosil Buckyprep column (4.6 ϕ \times 250 mm) with an eluent of 50% MeOH/CHCl₃ at 40 °C at a flow rate of 1.0 mL/min, and by combustion elemental analysis. IR spectra were recorded on an FT-IR and reported as wavenumbers (ν) in cm⁻¹. Proton (¹H) and carbon (¹³C) nuclear magnetic resonance (NMR) spectra were recorded at 400 and 100 MHz, respectively. Chemical shift values were given in ppm relative to internal oDCB-*d*₄ (for ¹H NMR: δ 7.19) or CDCl₃ (for ¹H NMR: δ 7.26; for ¹³C NMR: δ 77.16). The ¹H NMR spectral data are reported as follows: chemical shift, multiplicity (*s* = singlet, *d* = doublet, *t* = triplet), coupling constants (Hz), and integration. Time-of-flight mass spectra (TOF-MS) and high resolution mass spectra (HRMS) were obtained using matrix-assisted laser desorption ionization (MALDI) with tetracyanoquinodimethane (TCNQ) as the matrix. Structures of isolated congeners were studied by X-ray diffraction analysis of single crystals. UV–visible absorption spectra were reported in CHCl₃ at room temperature. Decomposition temperatures were recorded on a thermogravimetry–differential thermal analysis–mass equipment (TG-DTA-MS). The samples were first equilibrated to 50 °C for 10 min and then heated at a constant rate of 10 °C/min in flowing helium.

Toluene and DMF were purified by a solvent purification system equipped with columns of activated alumina and supported copper catalyst (Q-5). 2,2'-Bipyridine was purified by recrystallization from hexane. *m*-Dibromobenzene, bis(1,5-cyclooctadiene)nickel(0), and 1,5-cyclooctadiene were used as purchased.

A Typical Procedure for Synthesis and Isolation. A mixture of 2,2'-bipyridine (26.5 g, 170 mmol), 1,5-cyclooctadiene (20.7 mL, 169 mmol), and bis(1,5-cyclooctadiene)nickel(0) (46.6 g, 169 mmol) in a mixture of degassed toluene (350 mL) and DMF (350 mL) was stirred at 80 °C for 50 min. To the mixture at 80 °C was added a solution of *m*-dibromobenzene (10.2 mL, 84.4 mmol) in toluene (1.40 L) dropwise over 1 h, and the mixture was stirred at 80 °C for an additional 1 h. After the reaction mixture was cooled down to ambient temperature, 1 M hydrochloric acid (1 L) was added. The mixture was stirred for overnight, and the crude mixture was separated into a toluene solution and precipitates. The toluene solution was washed with water and brine, dried over MgSO₄, and concentrated under vacuum to give crude materials (3.85 g) containing [5]-, [7]-, and [9]-[14]CMP (Figure S1, Supporting Information). From the mixture of congeners was first isolated [5]CMP in 17% yield (1.10 g, 2.89 mmol) through extraction with CHCl₃ (700 mL) and subsequent recrystallization from toluene. Next congeners isolated were [7]- and [9]CMP through GPC and recrystallization: [7]CMP was obtained in 7% yield (504 mg, 0.903 mmol) by recrystallization from CHCl₃/MeCN, and [9]CMP was obtained in 1% yield (65.8 mg, 0.0861 mmol) by recrystallization from toluene. The crude precipitates (3.58 g) contained [6]- and [8]CMP. [8]CMP was obtained in 1% yield (73.1 mg, 0.111 mmol) through extraction with PhCl (500 mL) and subsequent recrystallization from PhCl/MeOH. [6]CMP was isolated by a combination of two methods. The residual crude materials were dissolved in oDCB at 180 °C, and from the oDCB extracts was obtained 306 mg of [6]CMP by subsequent recrystallization from oDCB. From the residue was obtained 361 mg of [6]CMP by sublimation. In total, [6]CMP was obtained in 10% yield (667 mg, 1.46 mmol). Because of the highly insoluble nature of [6]- and [8]CMP, ¹H NMR spectra were recorded in nearly saturated solution at elevated temperature, and the ¹³C NMR spectra were not obtained.

[5]CMP. Obtained as white crystals in 17% yield, 1.10 g. IR (powder) 3046 (w), 1604 (w), 1567 (w), 1488 (w), 1391 (w), 1315 (w), 1164 (w), 1068 (w), 925 (w), 899 (w), 815 (w), 772 (s), 737 (w), 699 (m), 633 (m), 609 (w); ¹H NMR (400 MHz, CDCl₃, rt): δ 8.52 (t, *J* = 2.0 Hz, 5H), 7.73 (dd, *J* = 2.0, 7.6 Hz, 10H), 7.51 (t, *J* = 7.6 Hz, 5H); ¹³C NMR (100 MHz, CDCl₃, rt): δ 141.3, 134.6, 129.0, 124.2; *T*_d (onset) 358 °C (helium atmosphere); HRMS (MALDI-TOF) *m/z* calcd for C₃₀H₂₀ [M]⁺ 380.1560, found 380.1559; Anal. Calcd for C₃₀H₂₀ C: 94.70, H: 5.30, found C: 94.37, H: 5.45.

[6]CMP. Obtained as white crystals in 10% yield, 667 mg. IR (powder) 3035 (w), 1602 (w), 1573 (w), 1489 (w), 1396 (w), 1301 (w), 1176 (w), 1090 (w), 916 (w), 891 (w), 812 (w), 776 (s), 723

(w), 701 (m), 628 (m), 615 (w); ¹H NMR (400 MHz, oDCB-*d*₄, 100 °C): δ 8.18 (s, 6H), 7.63 (d, *J* = 7.6 Hz, 12H), 7.45 (t, *J* = 7.6 Hz, 6H); *T*_d (onset) 451 °C (helium atmosphere); HRMS (MALDI-TOF) *m/z* calcd for C₃₆H₂₄ [M]⁺ 456.1873, found 456.1873; Anal. Calcd for C₃₆H₂₄ C: 94.70, H: 5.30, found C: 94.69, H: 5.35.

[7]CMP. Obtained as white crystals in 7% yield, 504 mg. IR (powder) 3034 (w), 1603 (w), 1576 (w), 1485 (w), 1396 (w), 1300 (w), 1179 (w), 1092 (w), 924 (w), 893 (w), 885 (w), 805 (w), 786 (m), 774 (s), 702 (s), 644 (w), 627 (m); ¹H NMR (400 MHz, CDCl₃, rt): δ 8.04 (t, *J* = 2.0, Hz, 7H), 7.64 (dd, *J* = 2.0, 7.6 Hz, 14H), 7.55 (t, *J* = 7.6 Hz, 7H); ¹³C NMR (100 MHz, CDCl₃, rt): δ 141.8, 129.4, 126.7, 125.8; *T*_d (onset) 440 °C (helium atmosphere); HRMS (MALDI-TOF) *m/z* calcd for C₄₂H₂₈ [M]⁺ 532.2186, found 532.2185; Anal. Calcd for C₄₂H₂₈·0.04CHCl₃·0.5SCH₃CN C: 92.65, H: 5.34, N: 1.26, Cl: 0.76, found C: 92.38, H: 5.38, N: 1.26, Cl: 0.57.

[8]CMP. Obtained as white crystals in 1% yield, 73.1 mg. IR (powder) 3023 (w), 1603 (w), 1573 (w), 1481 (w), 1409 (w), 1397 (w), 1301 (w), 1167 (w), 1091 (w), 914 (w), 894 (w), 815 (w), 792 (s), 784 (s), 715 (w), 708 (m), 701 (m), 642 (w), 625 (m); ¹H NMR (400 MHz, oDCB-*d*₄, 100 °C): δ 7.80 (s, 8H), 7.43 (d, *J* = 6.8 Hz, 16H), 7.37 (t, *J* = 6.8 Hz, 8H); *T*_d (onset) 449 °C (helium atmosphere); HRMS (MALDI-TOF) *m/z* calcd for C₄₈H₃₂ [M]⁺ 608.2499, found 608.2499; Anal. Calcd for C₄₈H₃₂·0.28C₆H₅Cl·0.66CH₃OH C: 91.41, H: 5.49, N: 0.00, Cl: 1.50, found C: 91.02, H: 5.25, N: 0.36, Cl: 1.11.

[9]CMP. Obtained as white crystals in 1% yield, 65.8 mg. IR (powder) 3053 (w), 1598 (w), 1576 (w), 1472 (w), 1400 (w), 1387 (w), 1168 (w), 1091 (w), 892 (w), 806 (w), 787 (s), 782 (s), 728 (w), 707 (s), 629 (w), 619 (w); ¹H NMR (400 MHz, CDCl₃, rt): δ 7.77 (t, *J* = 1.6 Hz, 9H), 7.57 (dd, *J* = 1.6, 7.6 Hz, 18H), 7.51 (t, *J* = 7.6 Hz, 9H); ¹³C NMR (100 MHz, CDCl₃, rt): δ 141.8, 129.0, 126.6, 126.3; *T*_d (onset) 480 °C (helium atmosphere); HRMS (MALDI-TOF) *m/z* calcd for C₅₄H₃₆ [M]⁺ 684.2812, found 684.2810; Anal. Calcd for C₅₄H₃₆·0.8C₇H₈·0.3H₂O C: 93.70, H: 5.67, found C: 93.48, H: 5.65, N: 0.13.

■ ASSOCIATED CONTENT

● Supporting Information

Physical data (MS, NMR, HPLC, UV–vis absorption, and thermogravimetric analysis), X-ray crystallographic analysis, and theoretical calculations for all isolated [*n*]CMP, and OLED device performance. This material is available free of charge via the Internet at <http://pubs.acs.org>.

■ AUTHOR INFORMATION

Corresponding Authors

*E-mail: satosota@m.tohoku.ac.jp.

*E-mail: isobe@m.tohoku.ac.jp.

Notes

The authors declare no competing financial interest.

■ ACKNOWLEDGMENTS

This study was partly supported by KAKENHI (24241036, 25107708, 25102007) and the Asahi Glass Foundation. We thank Dr. M. Oinuma and Mr. H. Seki for the large-scale preparation of CMP for the device applications and Mr. H. Kiso for his help with the device fabrications.

■ REFERENCES

- (1) Iyoda, M.; Yamakawa, J.; Rahman, M. J. *Angew. Chem., Int. Ed.* **2011**, *50*, 10522–10553.
- (2) For [4]COP, see: (a) Rapson, W. S.; Shuttleworth, R. G.; van Niekerk, J. N. *J. Chem. Soc.* **1943**, 326–327. (b) Irngartinger, H.; Reibel, W. R. K. *Acta Crystallogr. B* **1981**, *37*, 1724–1728. For [6] COP, see: (c) Wittig, G.; Rümpler, K.-D. *Liebigs Ann. Chem.* **1971**, *751*, 1–16. (d) Irngartinger, H. *Isr. J. Chem.* **1972**, *10*, 635–647.

(e) Ernst, L.; Mannschreck, A.; Rümpler, K.-D. *Org. Magn. Reson.* **1973**, *5*, 125–128.

(3) For the nomenclature of phenylene macrocycles, we adopted a system that became popular after the synthesis of CPP.

(4) (a) Staab, H. A.; Binnig, F. *Tetrahedron Lett.* **1964**, *5*, 319–321.

(b) Staab, H. A.; Binnig, F. *Chem. Ber.* **1967**, *100*, 293–305.

(5) (a) Cram, D. J.; Kaneda, T.; Helgeson, R. C.; Lein, G. M. *J. Am. Chem. Soc.* **1979**, *101*, 6752–6754. (b) Cram, D. J.; Kaneda, T.; Helgeson, R. C.; Brown, S. B.; Knobler, C. B.; Maverick, E.; Trueblood, K. N. *J. Am. Chem. Soc.* **1985**, *107*, 3645–3657.

(6) Pisula, W.; Kastler, M.; Yang, C.; Enkelmann, V.; Müllen, K. *Chem.—Asian J.* **2007**, *2*, 51–56.

(7) Chan, J. M. W.; Swager, T. M. *Tetrahedron Lett.* **2008**, *49*, 4912–4914.

(8) (a) Jasti, R.; Bhattacharjee, J.; Neaton, J. B.; Bertozzi, C. R. *J. Am. Chem. Soc.* **2008**, *130*, 17646–17647. (b) Takaba, H.; Omachi, H.; Yamamoto, Y.; Bouffard, J.; Itami, K. *Angew. Chem., Int. Ed.* **2009**, *48*, 6112–6116. (c) Yamago, S.; Watanabe, Y.; Iwamoto, T. *Angew. Chem., Int. Ed.* **2010**, *49*, 757–759.

(9) (a) Nakanishi, W.; Yoshioka, T.; Taka, H.; Xue, J. Y.; Kita, H.; Isobe, H. *Angew. Chem., Int. Ed.* **2011**, *50*, 5323–5326. (b) Nakanishi, W.; Xue, J. Y.; Yoshioka, T.; Isobe, H. *Acta Crystallogr., Sect. E: Struct. Rep. Online* **2011**, *E67*, o1762–o1763. (c) Xue, J. Y.; Nakanishi, W.; Tanimoto, D.; Hara, D.; Nakamura, Y.; Isobe, H. *Tetrahedron Lett.* **2013**, *54*, 4963–4965.

(10) For other examples of our π -extended cycloarylenes, see: (a) Matsuno, T.; Naito, H.; Hitosugi, S.; Sato, S.; Kotani, M.; Isobe, H. *Pure Appl. Chem.* **2014**, *86*, 489–495. (b) Matsuno, T.; Kamata, S.; Hitosugi, S.; Isobe, H. *Chem. Sci.* **2013**, *4*, 3179–3183. (c) Isobe, H.; Hitosugi, S.; Yamasaki, T.; Iizuka, R. *Chem. Sci.* **2013**, *4*, 1293–1297. (d) Hitosugi, S.; Yamasaki, T.; Isobe, H. *J. Am. Chem. Soc.* **2012**, *134*, 12442–12445. (e) Hitosugi, S.; Nakanishi, W.; Isobe, H. *Chem.—Asian J.* **2012**, *7*, 1550–1552. (f) Hitosugi, S.; Nakanishi, W.; Yamasaki, T.; Isobe, H. *Nat. Commun.* **2011**, *2*, 492. (g) Nakanishi, W.; Matsuno, T.; Ichikawa, J.; Isobe, H. *Angew. Chem., Int. Ed.* **2011**, *50*, 6048–6051.

(11) McKinnon, J. J.; Spackman, M. A.; Mitchell, A. S. *Acta Crystallogr., Sect. B: Struct. Sci.* **2004**, *B60*, 627–668.

(12) Staab and co-workers reported four different methods for the synthesis of [6]CMP as the major congener (ref 4). Yields of major [6]CMP from *m*-dibromobenzene with a single phenylene unit were as follows: 1 \times 6 macrocyclization of the “phenyl” magnesium bromide with CuCl₂ = 1.1% yield, 2 \times 3 macrocyclization of “biphenyl” magnesium bromide with CuCl₂ = 4.4% yield, 3 \times 2 macrocyclization of “terphenyl” magnesium bromide with CuCl₂ = 5.4% yield, intramolecular macrocyclization of “hexaphenyl” magnesium bromide with CuCl₂ = 5.8% yield. The yield of [8]CMP was recorded from biphenyl and was 0.72% from *m*-dibromobenzene.

(13) Cram and co-workers reported a six-step synthesis of highly substituted [6]CMP (known as spherand) in 6% yield (ref 5).

(14) Müllen and co-workers reported a five-step synthesis of trimethylsilyl-substituted [6]CMP from 1,3,5-tribromobenzene (ref 6). The total yield of trimethylsilyl-substituted [6]CMP was 30%.

(15) Swager and co-workers reported Suzuki cross-coupling synthesis of highly functionalized [6]CMP with the yield of 13% (ref 7).

(16) (a) Yamamoto, T. *Prog. Polym. Sci.* **1992**, *17*, 1153–1205. (b) Yamamoto, T.; Hayashi, Y.; Yamamoto, A. *Bull. Chem. Soc. Jpn.* **1978**, *51*, 2091–2097.

(17) The major difference between original polymerization conditions and the present conditions is the concentration of the substrate. Yamamoto used a high concentration of 1 M for the polymerization, and we used a diluted concentration of 40 mM for the cyclization.

(18) Although we used our own data in the structural analysis, molecular structures from X-ray diffraction analysis for [5]- and [6] CMP have been reported: (a) Irgartinger, H.; Leiserowitz, L.; Schmidt, G. M. J. *Chem. Ber.* **1970**, *103*, 1132–1156. (b) Irgartinger, H.; Leiserowitz, L.; Schmidt, G. M. J. *J. Chem. Soc. B* **1970**, 497–504.

(19) Wolff, S. K.; Grimwood, D. J.; McKinnon, J. J.; Turner, M. J.; Jayatilaka, D.; Spackman, M. A. *CrystalExplorer, version 3.1.1*; University of Western Australia, 2012.

(20) Sato, S.; Yamasaki, T.; Isobe, H. *Proc. Natl. Acad. Sci. U. S. A.* **2014**, *111*, 8374–8379.

(21) Miyahara, T.; Shimizu, M. *J. Cryst. Growth* **2001**, *229*, 553–557.

(22) (a) Hummer, G.; Rasaiah, J. C.; Noworyta, J. P. *Nature* **2001**, *414*, 188–190. (b) Koga, K.; Gao, G. T.; Tanaka, H.; Zeng, X. C. *Nature* **2001**, *412*, 802–805.

(23) (a) Koshino, M.; Tanaka, T.; Solin, N.; Suenaga, K.; Isobe, H.; Nakamura, E. *Science* **2007**, *316*, 853. (b) Koshino, M.; Solin, N.; Tanaka, T.; Isobe, H.; Nakamura, E. *Nat. Nanotechnol.* **2008**, *3*, 595–597.

(24) This observation is very similar to that observed for [n]CNAP (ref 9).

(25) Melting temperature analysis of Staab showed the decomposition temperature of [6]CMP to be above 500 °C (ref 4).

(26) [n]CNAP possessed higher strain energies, but their T_d values were higher (>500 °C).

(27) Yersin, H. *Highly Efficient OLEDs with Phosphorescent Materials*; Wiley: Darmstadt, 2008.

(28) Berresheim, A. J.; Müller, M.; Müllen, K. *Chem. Rev.* **1999**, *99*, 1747–1785.

(29) Ohta, E.; Sato, H.; Ando, S.; Kosaka, A.; Fukushima, T.; Hashizume, D.; Yamasaki, M.; Hasegawa, K.; Muraoka, A.; Ushiyama, H.; Yamashita, K.; Aida, T. *Nat. Chem.* **2011**, *3*, 68–73.

(30) Hawker, C. J.; Wooley, K. L. *Science* **2005**, *309*, 1200–1205.

(31) (a) Iwamoto, T.; Watanabe, Y.; Sadahiro, T.; Haino, Y.; Yamago, S. *Angew. Chem., Int. Ed.* **2011**, *50*, 8342–8344. (b) Xia, J.; Bacon, J. W.; Jasti, R. *Chem. Sci.* **2012**, *3*, 3018–3021.

(32) Zabula, A. V.; Filatov, A. S.; Xia, J.; Jasti, R.; Petrukhina, M. A. *Angew. Chem., Int. Ed.* **2013**, *52*, 5033–5036.

(33) (a) Golder, M. R.; Wong, B. M.; Jasti, R. *Chem. Sci.* **2013**, *4*, 4285–4291. (b) Kayahara, E.; Kouyama, T.; Kato, T.; Takaya, H.; Yasuda, N.; Yamago, S. *Angew. Chem., Int. Ed.* **2013**, *52*, 13722–13726.